Geochemistry of volcanic rocks in the Snowshoe Group (Neoproterozoic-Cambrian) and geochronology, Sm-Nd isotopic data, and geochemistry of crosscutting Permian intrusions: Episodic back-arc magmatism along the western edge of Ancestral North America in Kootenay terrane

Filippo Ferri[1, a], and Richard Friedman[2]

[1] Emeritus Scientist, British Columbia Geological Survey, Ministry of Mining and Critical Minerals, Victoria, BC, V8W 9N3
[2] Pacific Centre for Isotopic and Geochemical Research, Earth and Ocean Sciences, The University of British Columbia, Vancouver, BC, V6T 1Z4
[a] corresponding author: Filippo.Ferri@gov.bc.ca

Recommended citation: Ferri, F., and Friedman, R., 2026. Geochemistry of volcanic rocks in the Snowshoe Group (Neoproterozoic-Cambrian) and geochronology, Sm-Nd isotopic data, and geochemistry of crosscutting Permian intrusions: Episodic back-arc magmatism along the western edge of Ancestral North America in Kootenay terrane. In: Geological Fieldwork 2025, British Columbia Ministry of Mining and Critical Minerals, British Columbia Geological Survey Paper 2026-01, pp. 203-219.

Abstract

Vintage multigrain U-Pb zircon analysis on three samples of gabbro intruding late Neoproterozoic to Early Cambrian rocks of the Snowshoe Group collected in 2001 from Kootenay terrane (Cariboo subterrane) returned ages of ca. 280 Ma. Geochemical and isotopic data define two suites. One displays elemental levels suggesting derivation from an E-MORB and OIB (within-plate) source and has Sm-Nd isotopic abundances indicating the magmas originated from an immature mantle source. The second suite displays arc-like signatures and Sm-Nd isotopic levels that suggest derivation from more evolved continental lithosphere. These results are consistent with a Permian back-arc along the western margin of Ancestral North America. Lithogeochemical analysis of mafic volcanic rocks in the Snowshoe Group are predominantly alkali basalts indicating a within-plate setting, but some contain basalt to alkali basalt with both E-MORB and arc signatures, and others are alkali basalts displaying within-plate abundances. These results are consistent with an earlier, Neoproterozoic to Cambrian, back-arc.

Keywords: Snowshoe Group, Kootenay terrane, Cariboo subterrane, geochronology, Sm-Nd isotopes, Permian

1. Introduction

In the early 2000s, the British Columbia Geological Survey conducted systematic mapping in the Cariboo Lake area of Kootenay terrane focused on sulphide-bearing mafic volcanic rocks of the Snowshoe Group (Fig. 1), a succession of polydeformed and metamorphosed Neoproterozoic to lower Cambrian siliciclastic, carbonate, and volcanic rocks (Ferri, 2001a, b; Ferri and O'Brien, 2002, 2003). This paper presents previously unpublished multigrain U-Pb zircon ages and Sm-Nd isotopic data from three gabbroic intrusions that cut the Snowshoe Group, together with trace and rare earth element data from a regional suite of mafic to intermediate volcanic samples collected during this mapping. Geochronological data from the three samples return, within error, the same Early Permian age (ca. 280 Ma). Geochemical data from both the Snowshoe Group and crosscutting Permian intrusions are consistent with back-arc basin processes near the western flank of Ancestral North America.

2. Previous work

Our work in the region builds on numerous previous studies. Höy and Ferri (1998a, b) described mineralization in the Wells-Barkerville area, Ferri et al. (1999) detailed the age and geochemistry of the Quesnel Lake gneiss, Bichler and Bobrowski (2001) conducted a till geochemistry survey, and Ray et al. (2001) detailed the geochemistry of mineral deposits in the Wells-Barkerville area. Earlier investigations include Struik (1986, 1988), Campbell (1978), Rees (1987), and Rees and Ferri (1983). Schiarizza and Ferri (2003) and Ferri and Schiarizza (2006) redefined Snowshoe Group stratigraphy based on the recognition of large nappe-like structures that repeat stratigraphy. Investigations of adjoining rocks in Quesnel terrane include Struik (1983a, b), Bloodgood (1990), Panteleyev et al. (1996), and Schiarizza (2024).

3. Geological setting

Straddling the boundary between the Intermontane and Omineca morphotectonic belts, the Cariboo Lake area is in

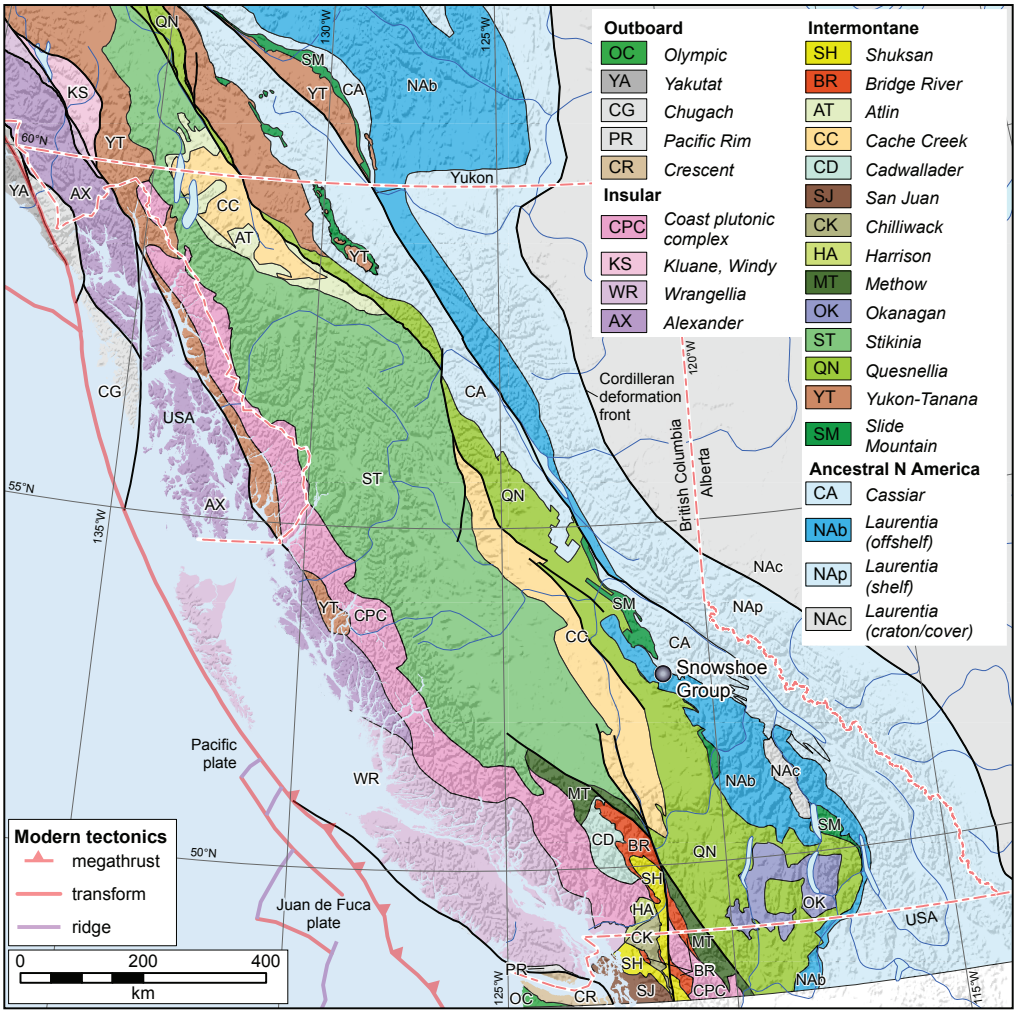

Fig. 1. Tectonic elements of the Canadian Cordillera in British Columbia and location of study area. Terranes after Colpron (2020).

Kootenay terrane, locally represented by Barkerville subterrane (Fig. 2). The Snowshoe Group (Neoproterozoic-lower Cambrian), which consists predominantly of siliciclastic rocks with lesser carbonate and volcanic rocks, represents part of the Ancestral North America clastic wedge that was displaced from the original continental margin. The unit is bounded to the southwest, across the northeast-vergent Eureka thrust, by Late Triassic to Early Jurassic arc volcanic rocks and comagmatic intrusions and siliciclastic rocks of Quesnel terrane (Nicola Group) and late Paleozoic oceanic rocks of Slide Mountain terrane (Crooked amphibolite). To the northeast, across the southwest-vergent Pleasant Valley thrust, are siliciclastic and carbonate rocks of the Cariboo terrane that originated closer to the Ancestral North American continental margin. To the north is a large Slide Mountain terrane klippe consisting of fine-grained siliciclastic rocks, chert, basalt, and mafic intrusive rocks (Slide Mountain Group). The klippe is floored by the Pundata thrust, which is considered to link with the Eureka thrust (Fig. 2; Ferri and O'Brien, 2003).

In the Jurassic-Cretaceous, the Snowshoe Group was polydeformed and metamorphosed to upper amphibolite grade. Ferri and O'Brien (2003) recognized a series of second-phase southwest-vergent nappes (Fig. 3), which enabled simplifying Snowshoe Group stratigraphy (Fig. 4; see also Schiarizza and Ferri, 2003; Ferri and Schiarizza, 2006). Mafic to intermediate volcanic rocks and small gabbroic dikes and sills are interspersed throughout the Snowshoe Group (Fig. 4). The most areally extensive volcanic rocks are exposed along the ridge containing Mount Barker and continuing northwest across the Cariboo River valley (Fig. 3). Grouped with this unit is a belt of doubly folded mafic metavolcanic rocks between Keithley and Rollie creeks (Fig. 3). Mafic to intermediate volcanic rocks are also found southwest of Frank Creek and near Badger Peak. Isolated mafic volcanic rocks also occur throughout the Harveys Ridge succession. Gabbroic dikes and sills are most prevalent in the Downey and Transitional Harveys successions near Keithly and Rollie creeks and in the Downie succession northeast of Mount Barker, one of which forms a mappable unit northeast of Mount Barker (Fig. 3). Two of the samples collected for U-Pb zircon geochronology are from this intrusion; the third is from a smaller sill between Rollie and Keithley creeks (Fig. 3).

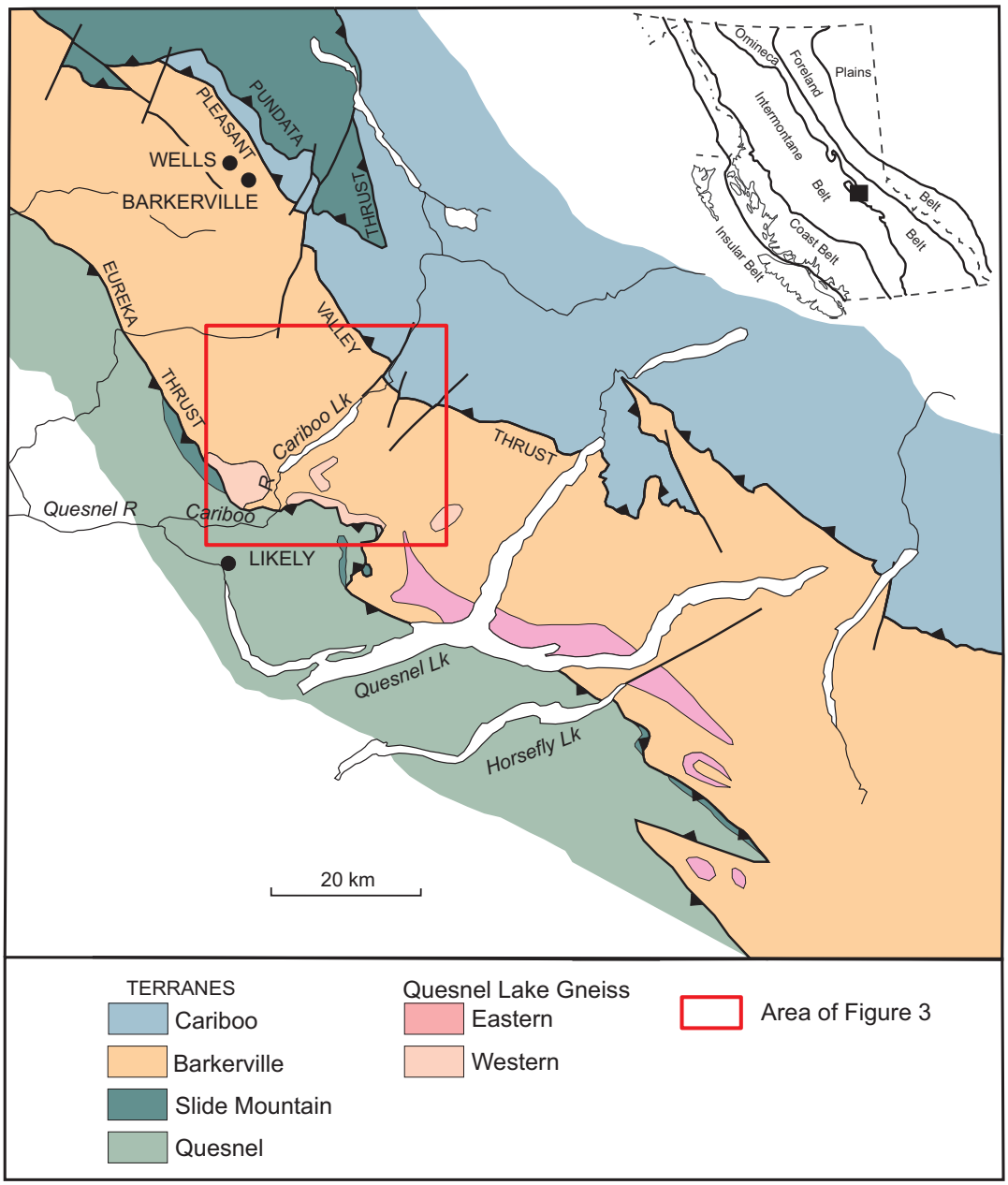

Fig. 2. Regional geological map. Modified after Struik (1986).

4. U-Pb zircon geochronology

During 2001 mapping, three gabbroic intrusions were sampled for geochronological analysis: two from a northwest-trending body northeast of Mount Barker and one from a sill intruding the Transitional Harveys Ridge succession between Rollie and Keithley creeks (Fig. 3). These bodies were chosen as they were relatively coarser grained and contained a few per cent modal quartz.

4.1. Analytical techniques

U-Pb geochronological analysis of the three samples began in late 2001. Multigrain zircon fractions were selected on the basis of zoning patterns observed in cathode luminescence and backscatter images. The portions of grains selected for analysis were broken off and plucked from grain mounts with a probe and surgical forceps under a binocular microscope. These fragments were air abraded before dissolution using the technique of Krogh (1982). This was followed by washing with 3N HNO_3 in an ultrasonic cleaner for 10 minutes and rinsing with deionized water and acetone. Immediately before dissolution, grain fragments were washed in clean 10 ml borosilicate beakers, with ultrapure 3N HNO_3 at 50°C for 20 minutes and rinsed with ultrapure water and sub-boiled acetone. Fragments were tapped onto Al-foil weigh boats and weighed on a Mettler M3

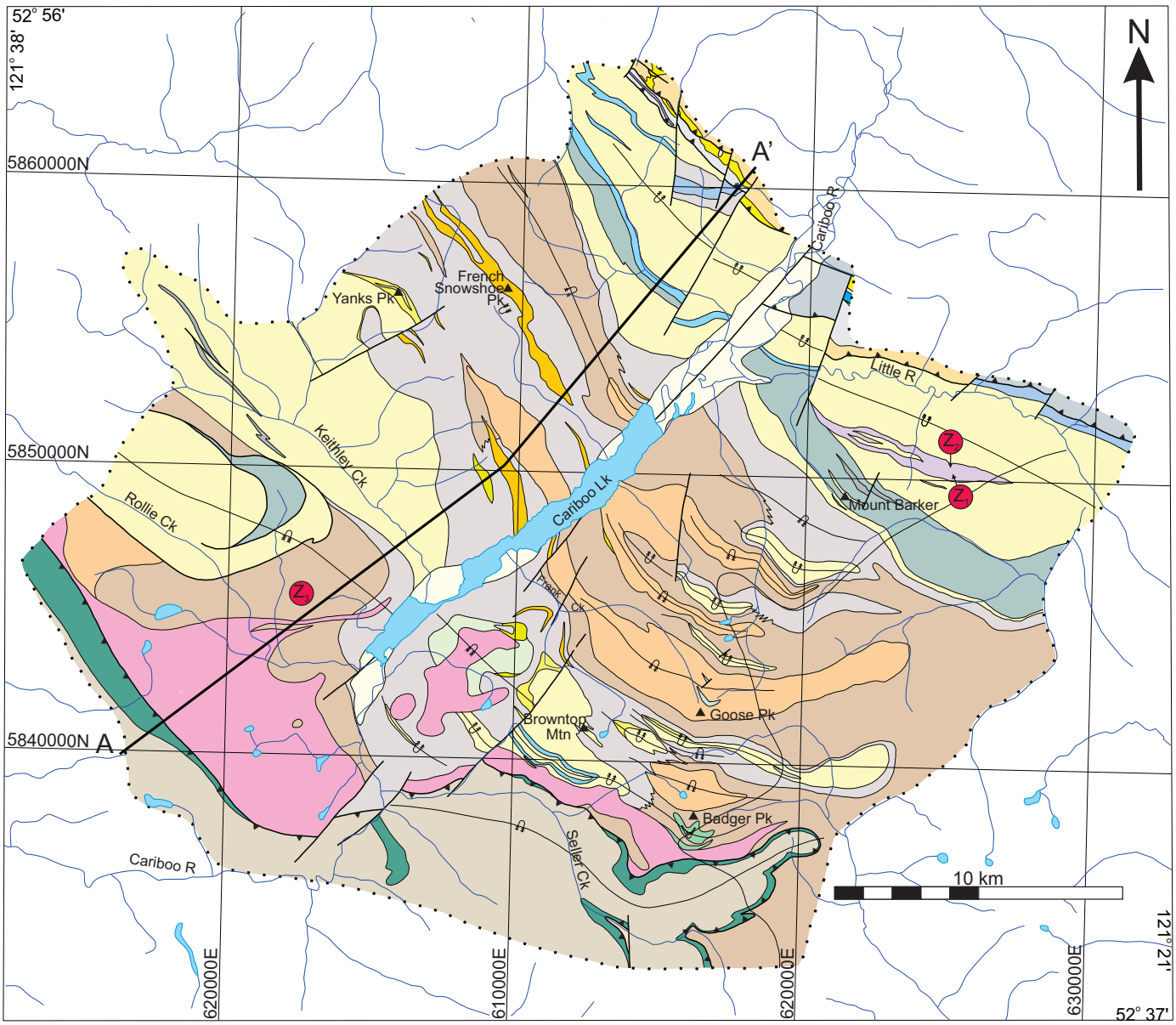

Fig. 3. a) Geology of the Cariboo Lake area. **b)** Legend.

microbalance with an estimated precision of ±2 mg and then loaded into 300 ml teflon or Savillex® PFA Parrish-style microcapsules. Zircon fragments were dissolved in ~100 ml of sub-boiled 29N HF and ~15 ml of sub-boiled 15N HNO_3 in the presence of a mixed $^{233\text{-}235}U$-^{205}Pb tracer for 40 hours at 240°C. Dissolution took place in conventional stainless steel Parr bombs with 250 ml teflon liners, each containing 8-13 microcapsules. Sample solutions were then dried to salts at ~125°C. Approximately 100 ml of ultrapure 3.1N HCl (sub-boiled 6.2N HCl + ultrapure water) was added to microcapsules, which were rebombed and salts were dissolved for 12 hours at 210°C. Separation and purification of Pb and U employed ion exchange column techniques modified slightly from those described by Parrish et al. (1987), using 250 ml resin volume FEP shrink tube columns. Pb and U were eluted sequentially into the same 7 ml Savillex® screwtop beaker followed by the addition of ~10 ml of 0.6N ultra-pure phosphoric acid. Each sample was loaded onto a single zone refined Re filament using a phosphoric acid-silica gel emitter made with silicon tetrachloride. Isotopic ratios were measured using a modified single collector VG-54R thermal ionization mass spectrometer equipped with a Daly photomultiplier. Both U and Pb were run at 1450°C, in peak-switching mode on the Daly detector. U fractionation was determined directly on individual runs using the $^{233\text{-}235}U$ tracer, and Pb isotopic ratios were corrected for a fractionation of 0.37%/amu, based on replicate analyses of the NBS-981 Pb standard and the values recommended by Thirlwall (2000). U and Pb analytical blanks were less than 1 pg and in

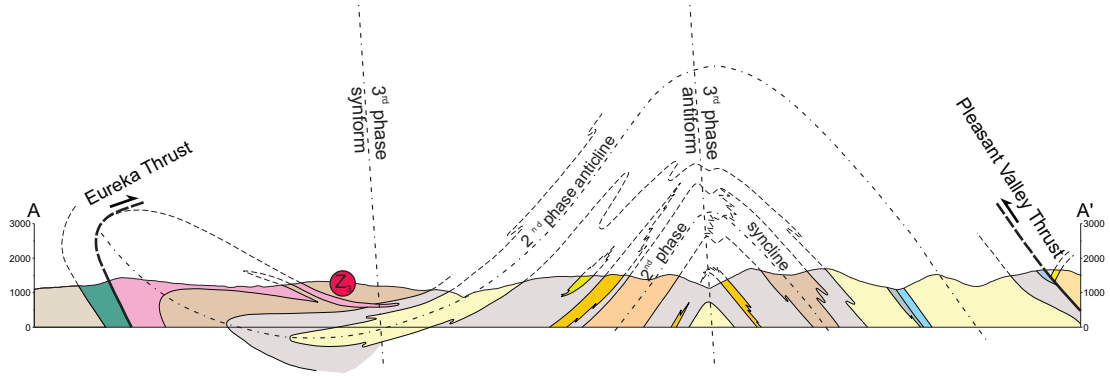

Slide Mountain terrane

Quaternary

M. to L. Triassic
SLOCAN GP
Dark grey to black phyllite

Penn. to Permian
SLIDE MOUNTAIN GP
Crooked amphibolite; chlorite schist, amphibolite ultramafite

Kootenay terrane

E. Permian
Gabbro

E. Mississippian
Western Quesnel Lk gneiss; mega crystic orthogneiss

Proterozoic and Cambrian
SNOWSHOE GP
Cambrian
Bralco limestone
Grey to cream limestone

Goose Peak quartzite
Quartzite and quartzite conglomerate

Chloritic phyllite to schist

Agnes conglomerate
Granule to boulder conglomerate

Harveys Ridge succession
Grey to dark grey phyllite

Transitional Harveys Ridge; grey to dark grey phyllite, sandstone.

Frank Creek mafic to intermediate metavolcanic rocks;

Frank Creek mafic metavolcanic rocks

Badger Peak mafic metavolcanic rocks

Neoproterozoic to Cambrian
Downey succession
Quartzite

Micaceous to feldspathic sandstone

Chlorite schist (meta-volcanics)

Dark grey limestone

Grey to white limestone

Neoproterozoic or Cambrian
SNOWSHOE GP undivided

Cariboo terrane

Permian?
Gabbro

L. Ordovician and Devonian or younger
BLACK STUART GP
Black shale, argillite, limestone

Proterozoic and Paleozoic
CARIBOO Gp
Cariboo Gp undivided

E. Cambrian
Midas Fm

Yanks Peak Fm

Neoproterozoic
Yankee Belle Fm

Second phase anticline, syncline

Third phase antiform, synform

Z U-Pb geochronology sample

Fig. 3. b) Legend.

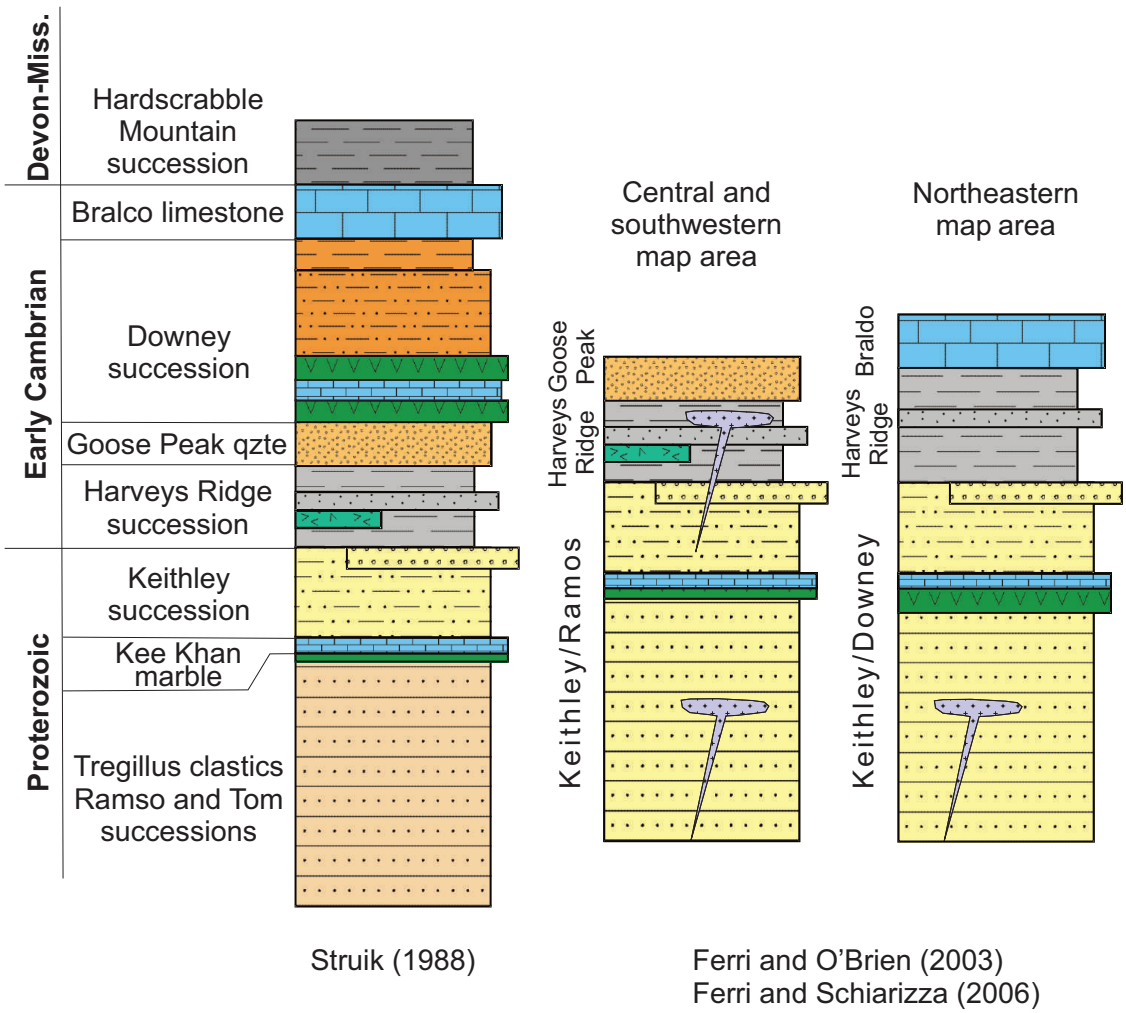

Fig. 4. Generalized stratigraphy of the Snowshoe Group as proposed by Struik (1988) and re-interpretation by Ferri and O'Brien (2003) and Ferri and Schiarizza (2006) based on repetition of units in large F_2 folds.

the range of 1.5-3.5 pg, respectively, during the course of this study. Common Pb isotopic compositions are derived from the model of Stacey and Kramers (1975). Concordia intercept ages and associated errors were calculated using a modified version of the York-II regression model (wherein the York-II errors are multiplied by the MSWD) and the algorithm of Ludwig (1980). All ages are quoted at the 2σ level of uncertainty. Isotopic dates are calculated with the decay constants λ238 = 1.55125E-10 and λ235 = 9.8485E-10 (Jaffey et al., 1971).

4.2. Results

Data from all three multigrain samples (Table 1) indicate significant lead loss; sample BO-06-04 also indicates evidence of inheritance. Regression lines on concordia plots yield upper intercepts that suggest a single crystallization age of ca. 280 Ma (Fig. 5).

5. Lithogeochemistry

Rare earth element data for more than 50 samples of mafic to intermediate metavolcanic and mafic intrusive rocks (Table 2) were determined at Memorial University in St. John's, Newfoundland using peroxide fusion followed by inductively coupled plasma mass spectrometry (ICP-MS) analyses. The corresponding major oxide and trace element compositions for many of these samples are provided in Ferri (2001a) and Ferri and O'Brien (2002). Whole rock Sm-Nd isotopic abundances for selected mafic intrusive bodies, including those analyzed for U-Pb geochronology (Table 3), were generated at the Pacific Centre for Isotopic and Geochemical Research, University of British Columbia in Vancouver.

Based on these analyses, we recognize three broad age groupings of igneous rocks (Fig. 6). One group consists of Mississippian to Permian metavolcanic rocks of the Crooked amphibolite. The second includes several Permian intrusions: 1) a gabbro sill in rocks of Cariboo terrane; 2) gabbroic sills and dikes intruding Snowshoe Group rocks between

Table 1. Multigrain U-Pb zircon analyses.

	Compositional Parameters									Radiogenic Isotope Ratios									Isotopic Ages					
Sample	Wt. mg	U ppm	Th/U	Pb ppm	$^{206}Pb^*$ x10^{-13} mol	mol % $^{206}Pb^*$	Pb^*/Pb_c	Pb_c (pg)	$^{206}Pb/^{204}Pb$	$^{208}Pb/^{206}Pb$	$^{207}Pb/^{206}Pb$	% err	$^{207}Pb/^{235}U$	% err	$^{206}Pb/^{238}U$	% err	corr. coef.	$^{207}Pb/^{206}Pb$	±	$^{207}Pb/^{235}U$	±	$^{206}Pb/^{238}U$	±
(a)	(b)	(c)	(d)	(c)	(e)	(e)	(e)	(e)	(f)	(g)	(g)	(h)	(g)	(h)	(g)	(h)		(i)	(h)	(i)	(h)	(i)	(h)
01FFe39-1																								
A	0.014	14320	0.756	569.4	278.1437	97.79%	14	520.87	805	0.246	0.051745	1.541	0.237406	1.681	0.033275	0.222	0.670	274.17	35.30	216.29	3.27	211.01	0.46
B	0.011	12459	0.918	571.6	201.1978	96.09%	8	678.79	467	0.298	0.051912	0.539	0.252027	0.643	0.035211	0.299	0.553	281.55	12.33	228.22	1.31	223.08	0.65
C	0.013	9517	0.852	376.8	173.2806	99.02%	33	142.30	1859	0.278	0.051816	0.269	0.239983	0.541	0.033590	0.403	0.877	277.31	6.17	218.41	1.06	212.98	0.84
D	0.008	13331	1.046	583.1	154.5681	98.27%	20	224.96	1057	0.339	0.051730	0.322	0.247926	0.472	0.034760	0.237	0.783	273.48	7.37	224.89	0.95	220.27	0.51
E	0.009	9767	0.766	473.1	132.9370	94.13%	5	689.22	308	0.249	0.051997	1.826	0.260040	1.926	0.036271	0.379	0.357	285.26	41.74	234.70	4.04	229.68	0.85
01FFe39-2																								
A	0.007	13774	0.972	621.3	139.8978	96.67%	10	399.09	542	0.316	0.051825	1.096	0.248661	1.219	0.034799	0.262	0.555	277.70	25.08	225.49	2.46	220.51	0.57
B	0.023	2111	0.727	91.9	75.7651	98.40%	20	102.91	1115	0.235	0.051875	0.938	0.267701	1.051	0.037428	0.313	0.490	279.89	21.47	240.85	2.25	236.87	0.73
C	0.016	13362	0.900	567.6	313.2660	98.51%	22	393.80	1180	0.292	0.051714	1.374	0.250583	1.599	0.035143	0.592	0.539	272.79	31.48	227.05	3.25	222.66	1.29
D	0.016	11949	0.927	527.2	280.9968	97.55%	13	585.13	745	0.301	0.051891	0.391	0.252196	0.538	0.035249	0.279	0.716	280.60	8.94	228.36	1.10	223.32	0.61
E	0.019	8121	0.918	342.3	225.7390	98.89%	30	210.22	1642	0.298	0.051895	0.261	0.251055	0.502	0.035087	0.354	0.871	280.76	5.96	227.43	1.02	222.31	0.77
BO-06-04																								
A	0.005	460	1.530	32.0	4.3137	97.97%	21	7.43	889	0.637	0.071386	0.657	0.442824	0.805	0.044990	0.399	0.583	968.50	13.42	372.24	2.51	283.69	1.11
B	0.011	399	2.556	32.9	8.1341	97.30%	18	18.72	673	0.976	0.064388	0.429	0.394412	0.504	0.044427	0.262	0.526	754.40	9.06	337.59	1.45	280.21	0.72
C	0.010	369	3.310	27.1	5.9649	97.99%	26	10.14	902	1.064	0.051884	0.494	0.277254	0.568	0.038757	0.214	0.511	280.28	11.30	248.48	1.25	245.12	0.51
D	0.010	1211	3.141	91.5	18.8701	93.57%	8	107.40	284	1.016	0.052021	0.724	0.267986	0.697	0.037362	0.440	0.252	286.31	16.56	241.08	1.50	236.46	1.02

(a) A, B, etc. are labels for fractions composed of air abraded zircon grains.

(b) Fraction masses determined on Mettler M3 microbalance to ±2 micrograms.

(c) U and total Pb concentrations subject to uncertainty in fraction mass.

(d) Model Th/U ratio calculated from radiogenic $^{208}Pb/^{206}Pb$ ratio and $^{207}Pb/^{235}U$ age.

(e) Pb* and Pbc represent radiogenic and common Pb, respectively; mol % $^{206}Pb^*$ with respect to radiogenic, blank and initial common Pb.

(f) Measured ratio corrected for spike and fractionation only. Mass discrimination of 0.37%/amu based on analysis of NBS-982; all Daly analyses.

(g) Corrected for fractionation, spike, and common Pb; up to 300 pg of common Pb was assumed to be procedural blank: $^{206}Pb/^{204}Pb = 17.40 \pm 3.0\%$; $^{207}Pb/^{204}Pb = 15.80 \pm 2.0\%$; $^{208}Pb/^{204}Pb = 36.40 \pm 1.0\%$ (all uncertainties 1-sigma). Excess over blank was assigned to initial common Pb with S-K model Pb composition at 280 Ma.

(h) Errors are 2-sigma, propagated using the algorithms of Schmitz and Schoene (2007) and Crowley et al. (2007).

(i) Calculations are based on the decay constants of Jaffey et al. (1971). $^{206}Pb/^{238}U$ and $^{207}Pb/^{206}Pb$ ages corrected for initial disequilibrium in $^{230}Th/^{238}U$ using Th/U [magma] = 3.

(j) Corrected for fractionation, spike, and blank Pb only.

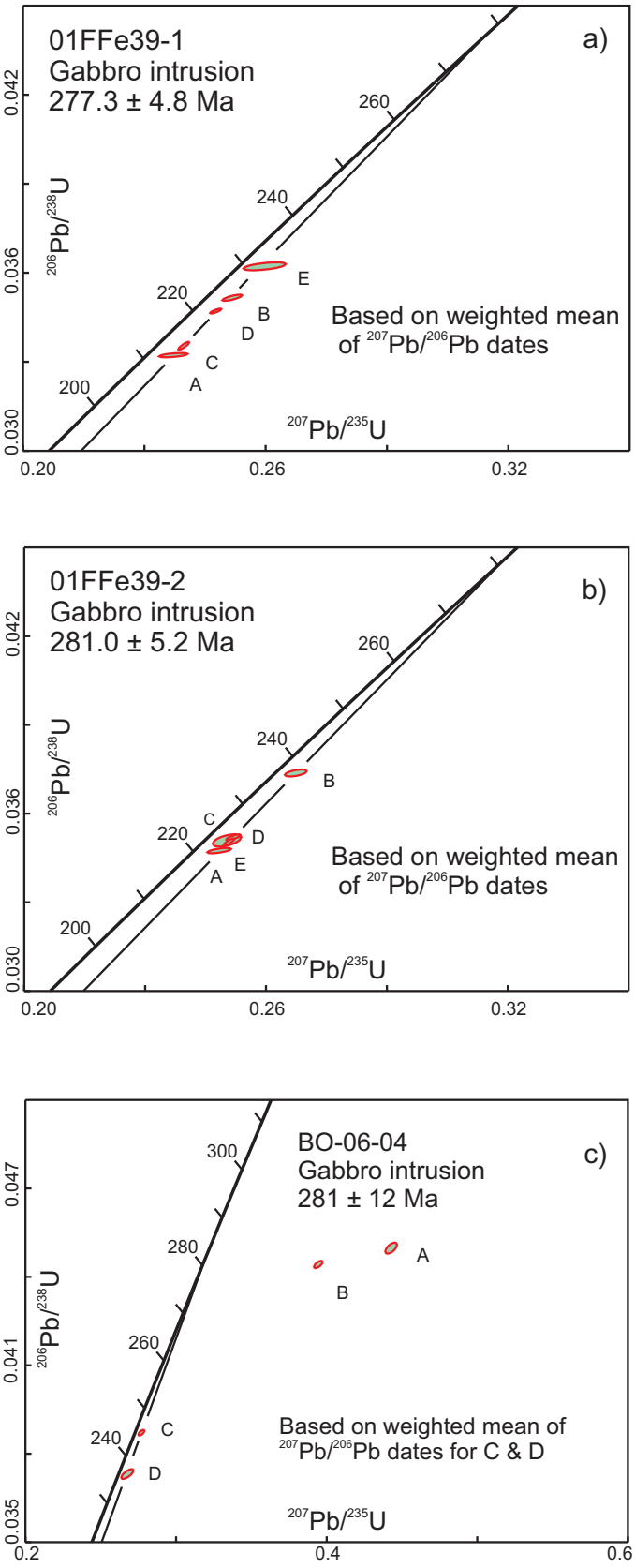

Fig. 5. Multigrain U-Pb zircon concordia plots for samples of gabbro that intrudes the Snowshoe Group north of Mount Barker (**a**, **b**) and northwest of southern Cariboo Lake (**c**).

Keithley and Rollie creeks; and 3) gabbroic intrusions in the Downey succession north of Mount Barker. The third includes Neoproterozoic to Cambrian metavolcanic rocks comprising: 1) metavolcanic rocks along Badger Peak; 2) metavolcanic rocks in the Harveys Ridge succession southwest of Frank Creek; 3) metavolcanic rocks in the Harveys Ridge succession north of Cariboo Lake; 4) sheared gabbro and metavolcanic rocks southwest of Keithley Creek; and 5) metavolcanic rocks along the ridge containing Mount Barker and that extend northwestward across the Cariboo River.

5.1. Mississippian to Permian

5.1.1. Crooked amphibolite

Metavolcanic rocks of the Crooked amphibolite consist primarily of chlorite schist to finely crystalline amphibolite. Analyzed samples define a cluster of basaltic composition (Fig. 6a). A tectonic discrimination diagram using Th/Yb versus Nb/Yb defines a cluster straddling the E-MORB-N-MORB transition along the mantle array corridor (Fig. 7a). The MORB nature of these samples is further exemplified by flat REE and extended-REE patterns (Figs. 8a, b).

5.2. Permian

5.2.1. Gabbro in Cariboo terrane

A gabboic sill intrudes rocks of the Midas Formation in the far northern part of the map area (Fig. 3). This body is an alkaline basalt (Fig. 6a) plotting near the OIB area of the MORB-OIB (Fig. 7b), which is supported by REE abundances (Figs. 8c, d). This sill has textural, modal and geochemical attributes similar to gabbro intruding Snowshoe rocks between Keithley and Rollie creeks and are assumed to be of the same age.

5.2.2. Gabbro sills and dikes intruding Snowshoe Group rocks between Keithley and Rollie creeks

Fine-grained gabbro sills and/or dikes up to 10s of m thick intrude rocks of the Downey, Harveys Ridge, and Transitional Harveys Ridge successions between Keithley and Rollie creeks. One of these was dated by U-Pb geochronology and returned an age of ca. 280 Ma. Based on similar textural, modal, and geochemical characteristics we consider that all are of the same age. These rocks form two bulk compositional clusters: basalt and alkali basalt (Fig. 6a). The basaltic rocks plot within the E-MORB portion of the MORB- OIB array whereas the alkali basalts plot near the OIB field, suggesting within-plate affinities (Fig. 7a). Similarly, the basaltic rocks display typical flat MORB profiles in extended REE plots whereas the alkali basalts show enrichment in the light rare earth elements and depletion in the heavy rare earth elements (Figs. 8e, f).

5.2.3. Gabbro intrusions in the Downey succession north of Mount Barker

Fine- to medium-grained gabbro sills and dikes intrude the Downey succession north of Mount Barker. Two samples from a large (~5 km long, up to 1 km wide), northwest-trending

Table 2. Rare earth element geochemistry of selected igneous rocks.

Station No.	Easting	Northing	Unit	Lithology	Th ppm	La ppm	Ce ppm	Pr ppm	Nd ppm	Sm ppm	Eu ppm	Gd ppm	Tb ppm	Dy ppm	Ho ppm	Er ppm	Tm ppm	Yb ppm	Lu ppm	Hf ppm	Ta ppm
00FFE-23-5	616125	5837760	BP	Chlorite schist	4.19	35.92	68.43	7.75	30.70	6.04	1.90	5.60	0.83	4.97	1.01	2.94	0.37	2.24	0.32	4.90	3.49
00FFE-23-6	616164	5837567	BP	Gabbro	1.01	9.56	19.58	2.42	10.53	2.36	0.73	2.37	0.35	2.11	0.43	1.23	0.16	0.95	0.14	2.13	1.08
00FFE-15-9	610828	5839105	CA	Chlorite schist	0.55	3.99	9.47	1.53	7.78	2.31	0.84	3.01	0.50	3.37	0.77	2.40	0.32	1.97	0.29	1.83	0.16
00FFE-22-1	614272	5835709	CA	Listwanite	0.48	4.79	12.53	2.01	10.47	3.39	1.23	4.32	0.75	5.04	1.12	3.52	0.47	3.00	0.45	2.99	0.22
00FFE-22-2	614538	5835485	CA	Amphibolite	0.23	5.08	15.77	2.62	14.25	4.72	1.71	6.02	1.03	6.91	1.51	4.71	0.63	3.89	0.58	4.49	0.34
00FFE-24-2	616084	5836461	CA	Amphibolite	0.58	6.73	16.38	2.61	13.33	4.29	1.62	5.60	0.94	6.28	1.38	4.39	0.59	3.76	0.56	3.78	0.30
01BO-29-5	614366	5863133	C-D	Gabbro	1.49	9.15	18.10	2.21	9.33	2.15	0.78	2.56	0.37	2.23	0.40	1.07	0.13	0.80	0.12	2.06	0.87
01BO-31-5	614857	5862407	C-D	Gabbro	1.87	10.27	20.23	2.44	10.53	2.54	0.93	3.06	0.43	2.57	0.47	1.19	0.15	0.92	0.15	2.47	1.01
00FFE-38-1	609864	5841876	FC	Meta-basalt	10.91	31.35	57.14	6.74	24.44	4.31	0.73	3.39	0.48	2.84	0.57	1.72	0.22	1.40	0.20	3.74	1.22
00FFE-4-1	607352	5844008	FC	Meta-basalt	13.35	45.10	77.34	9.48	33.40	5.57	0.72	3.93	0.53	2.99	0.58	1.78	0.24	1.48	0.22	2.75	1.03
00FFE-4-11	609883	5843781	FC	Meta-basalt	10.72	24.47	46.29	5.89	21.94	4.25	0.76	3.34	0.47	2.75	0.56	1.68	0.23	1.41	0.21	3.06	1.03
00FFE-4-14	609712	5842941	FC	Chlorite schist	2.98	19.12	40.56	4.99	20.76	4.73	1.52	4.61	0.67	3.89	0.76	2.19	0.27	1.66	0.25	4.11	2.19
00FFE-4-7	608730	5843209	FC	Meta-basalt	14.20	39.86	71.42	8.54	29.84	4.87	1.07	3.34	0.45	2.54	0.50	1.54	0.21	1.32	0.19	3.70	1.10
00FFE-8-10	610179	5844196	FC	Meta-basalt	2.30	17.91	35.72	4.32	17.55	3.85	0.76	3.58	0.51	2.96	0.57	1.61	0.20	1.19	0.17	3.33	1.22
00FFE-8-11	610090	5844241	FC	Meta-basalt	2.55	20.64	44.10	5.41	22.39	4.55	1.36	4.30	0.62	3.57	0.72	2.05	0.26	1.54	0.21	4.16	2.04
00FFE-8-2	608248	5844719	FC	Meta-basalt	11.94	37.20	66.91	7.88	27.31	4.43	0.81	3.15	0.42	2.43	0.49	1.51	0.20	1.26	0.18	2.97	0.87
00FFE-9-7	608683	5842293	FC	Meta-basalt	0.44	4.60	12.89	2.07	10.83	3.62	1.29	4.78	0.80	5.47	1.20	3.79	0.50	3.16	0.47	3.39	0.23
01FFE-08-08	608950	5849809	HR-V	Chlorite schist	2.24	18.07	36.99	4.78	20.69	4.53	1.55	4.56	0.66	3.76	0.67	1.74	0.23	1.40	0.19	3.47	1.50
01FFE-09-02a	605096	5844003	HR-V	Chlorite schist	2.59	15.16	28.71	3.28	12.79	2.42	0.85	2.46	0.38	2.26	0.44	1.20	0.17	1.08	0.16	2.30	1.56
01FFE-09-4a	605812	5845055	HR-V	Chlorite schist	4.02	28.65	57.81	7.09	29.35	6.00	1.76	5.93	0.86	4.89	0.88	2.31	0.31	1.88	0.26	5.79	2.91
01FFE-09-4b	605812	5845055	HR-V	Chlorite schist	2.86	24.30	41.76	4.45	16.43	2.86	0.44	2.59	0.37	2.05	0.36	0.96	0.13	0.79	0.11	3.81	2.67
01FFe-35-2	615548	5860691	HR-V	Meta-basalt	0.40	4.16	9.35	1.33	5.59	1.38	0.38	1.65	0.24	1.54	0.36	1.00	0.12	0.79	0.10	1.87	0.39
01FFE-11-08	601192	5849676	KC	Chlorite schist	4.59	35.42	70.66	8.50	34.94	7.40	2.39	6.68	0.98	5.47	0.95	2.49	0.33	2.02	0.30	7.31	4.56
01FFE-11-7a	601064	5850147	KC	Chlorite schist	3.24	24.32	48.74	5.96	24.67	4.98	1.48	4.87	0.70	3.94	0.70	1.83	0.24	1.45	0.20	4.46	3.05
01FFE-11-7b	601064	5850147	KC	Chlorite schist	3.09	20.98	42.80	5.25	22.25	5.26	1.73	5.10	0.77	4.43	0.79	2.13	0.28	1.76	0.26	5.46	3.40
01BO-6-4	601826	5848997	KR-D	Gabbro	0.32	3.33	9.35	1.61	8.39	2.94	1.01	3.93	0.70	4.82	1.00	2.84	0.40	2.65	0.38	3.05	0.20
01FFE-03-01	597750	5845225	KR-D	Gabbro	0.40	3.56	9.50	1.57	8.34	2.68	1.00	4.17	0.72	4.86	1.09	3.26	0.51	3.39	0.42	2.59	0.15
01FFE-03-01A	597750	5845225	KR-D	Gabbro	4.29	28.77	59.16	7.32	30.76	6.30	2.08	6.89	0.97	5.66	1.12	3.05	0.43	2.74	0.33	6.14	2.79
01FFE-03-07	597440	5846775	KR-D	Gabbro	2.71	17.67	37.38	4.69	20.05	4.33	1.47	4.82	0.69	3.99	0.79	2.13	0.30	1.89	0.23	4.21	1.82
01FFE-06-09	602549	5845117	KR-D	Gabbro	3.77	26.55	55.85	6.99	29.53	6.02	2.03	6.42	0.88	4.94	0.94	2.50	0.35	2.17	0.26	5.17	3.43
01FFE-07-02	602901	5846038	KR-D	Gabbro	0.63	2.32	5.82	0.90	4.71	1.52	0.58	2.23	0.40	2.79	0.60	1.85	0.28	1.88	0.29	2.09	0.14
01FFE-11-04	603458	5849443	KR-D	Gabbro	1.07	6.83	17.44	2.67	13.66	4.36	1.49	5.60	0.98	6.60	1.34	3.94	0.58	3.80	0.60	4.93	0.36
01FFe-40-7a	602880	5846012	KR-D	Gabbro	0.70	2.90	7.15	1.06	5.26	1.78	0.65	2.31	0.46	3.28	0.67	2.07	0.30	2.08	0.33	2.37	0.17
BO-06-6	603109	5845654	KR-D	Gabbro	2.86	24.34	52.85	6.63	27.63	5.93	2.12	5.22	0.74	4.09	0.70	1.82	0.24	1.44	0.21	5.15	2.51
01FFe-41-1a	596524	5856980	KR-D	Gabbro	0.68	8.92	22.56	3.36	17.06	5.25	1.98	6.52	1.09	7.20	1.40	4.08	0.56	3.83	0.55	5.71	0.59
01FFe-41-1b	596524	5856980	KR-D	Chlorite schist	3.80	24.70	46.50	5.24	20.75	4.07	1.50	3.87	0.62	3.92	0.75	2.17	0.29	2.02	0.29	3.60	2.56
00FFE-34-5	621233	5849302	MB-D	Gabbro	5.15	19.70	39.02	5.06	21.32	5.00	1.41	4.84	0.69	4.01	0.79	2.35	0.30	1.89	0.28	2.80	0.31
00FFE-35-2	621817	5849596	MB-D	Gabbro	4.17	16.35	32.90	4.21	17.90	4.21	1.07	4.09	0.59	3.44	0.69	2.05	0.27	1.65	0.24	2.48	0.28
01BO-33-3a	626161	5849138	MB-D	Gabbro	5.03	19.62	39.56	5.23	22.88	5.33	1.61	5.77	0.81	4.86	0.84	2.31	0.32	2.07	0.30	3.62	0.34
01FFe-38-5	627262	5848373	MB-D	Gabbro	2.98	11.46	23.52	3.08	13.29	3.16	1.01	3.38	0.46	2.82	0.49	1.28	0.18	1.23	0.18	2.16	0.17
01FFe-39-1	625052	5850254	MB-D	Gabbro	1.36	10.49	23.06	3.29	14.00	2.82	0.94	2.91	0.42	2.50	0.58	1.67	0.21	1.35	0.16	1.86	0.16
01FFe-39-2	624956	5850418	MB-D	Gabbro	3.68	24.75	52.23	7.01	29.14	5.31	1.42	4.84	0.66	3.86	0.91	2.59	0.35	2.25	0.28	3.81	0.39
BO-18-03a	624336	5849846	MB-D	Gabbro	3.97	22.75	56.23	8.47	38.17	7.65	2.86	8.00	1.10	6.34	1.47	3.83	0.50	2.82	0.35	5.20	0.50
BO-18-05	625052	5850070	MB-D	Meta-basalt	7.16	32.46	66.06	8.32	34.83	7.93	2.39	8.22	1.06	6.00	0.98	2.48	0.34	2.11	0.32	4.94	0.68
00FFE-34-4	621228	5849252	MB-V	Chlorite schist	4.13	16.21	32.77	4.27	18.04	4.32	1.31	4.20	0.59	3.40	0.66	1.95	0.25	1.56	0.24	2.35	0.25
00FFE-34-6	621300	5849441	MB-V	Chlorite schist	4.39	22.77	46.75	5.93	24.50	5.40	1.72	5.00	0.70	4.00	0.73	1.96	0.23	1.35	0.20	3.92	1.10
00FFE-34-8	621325	5849754	MB-V	Meta-tuff	2.64	22.80	48.82	6.21	25.89	5.84	1.91	5.48	0.78	4.48	0.86	2.46	0.31	1.86	0.27	4.90	1.89
00FFE-36-7	620252	5851854	MB-V	Chlorite schist	4.90	20.87	41.96	5.47	23.22	5.49	1.57	5.22	0.74	4.27	0.83	2.48	0.32	1.96	0.29	2.70	0.29
00FFE-6-1	618855	5852940	MB-V	Chlorite schist	1.15	10.85	23.95	3.09	13.07	2.93	0.82	2.78	0.39	2.26	0.44	1.26	0.16	0.94	0.13	2.42	0.83
01FFE-17-02	613025	5858272	MB-V	Meta-basalt	4.52	29.32	60.54	7.42	30.71	6.62	2.12	6.06	0.89	5.04	0.89	2.32	0.31	1.90	0.29	7.28	3.37
BO-15-7a	613981	5857068	MB-V	Meta-basalt	1.48	24.80	57.45	7.95	34.36	6.24	1.94	6.00	0.83	4.90	1.19	3.12	0.40	2.50	0.29	7.27	2.59

Positive ion mass spectrometry (ICP-MS) at Memorial University of Newfoundland laboratories.
BP - Badger Peak Volcanics; CA - Crooked Amphibolite; DV - Downey Volcanics; FC - Frank Creek Volcanics; HR - Harveys Ridge Volcanics; KC - Sheared metavolcanics and gabbro southwest of Keithley Creek; KR - Gabbro/diorite between Keithley and Rollie creeks; MB-D - Mount Barker Diorite; MB-V - Mount Barker Volcanics; C-D - Cariboo Terrane Diorite/gabbro

Table 3. Sm-Nd isotope data for gabbro intruding the Snowshoe Group.

Sample Number	Age(T) (Map)	Sm (ppm)	Nd (ppm)	$^{147}Sm/^{144}Nd$	$^{143}Nd/^{144}Nd$	Error ±2s	$\varepsilon_{Nd}(T)$[1]	$\varepsilon_{Nd}(0)$	T_{DM}[2] (Ga)
01FFe-03-01	280	3.00	8.98	0.2021	0.512967	0.000007	6.2	6.4	N/A
01BO-6-4	280	3.51	10.17	0.2085	0.513012	0.000005	6.9	7.3	N/A
01FFe-39-1	280	3.08	12.95	0.1437	0.512319	0.000007	-4.3	-6.2	N/A
01FFe-39-2	280	5.10	23.98	0.1287	0.512208	0.000008	-6.0	-8.4	1.71

LA-ICP-MS analysis at the Pacific Centre for Isotopic and Geochemical Research, University of British Columbia, Vancouver, BC

[1]Calculated using $^{143}Nd/^{144}Nd$ of chondrite reservoir (CHUR) = 0.512638 and $^{147}Sm/^{144}Nd$ = 0.1966 (Hamilton et al., 1983).

[2]Calculated using $^{143}Nd/^{144}Nd$ = 0.513163 and $^{147}Sm/^{144}Nd$ = 0.2137 for the depleted mantle (DM) reservoir (Goldstein et al., 1984).

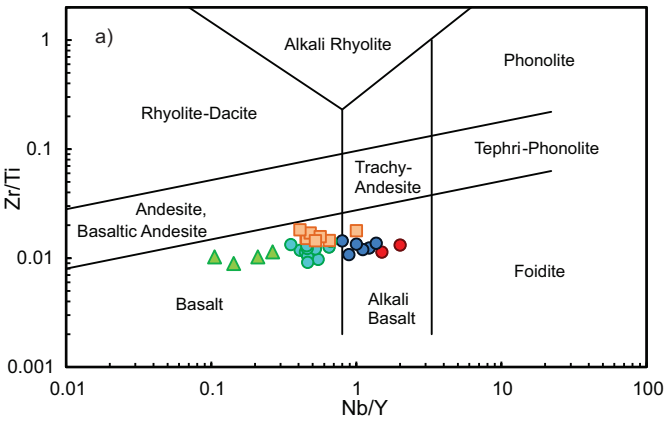

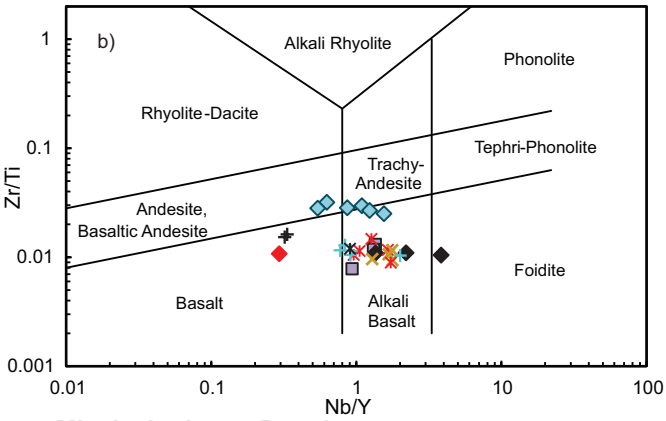

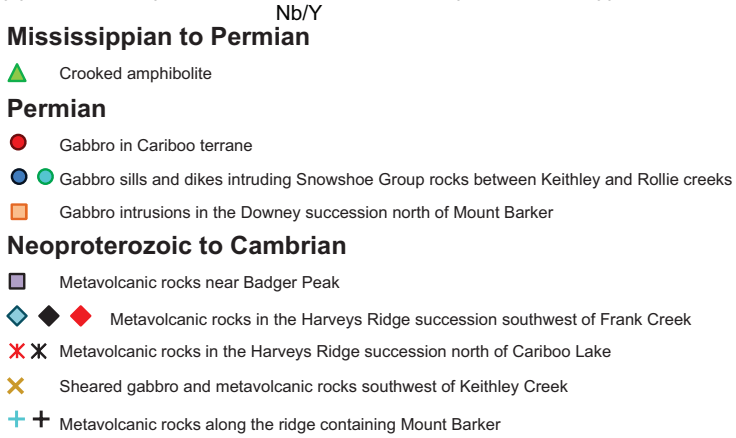

Fig. 6. Rock classification based on Zr/Ti vs. Nb/Y (Pearce, 1996). **a)** Mississippian to Permian rocks of the Crooked amphibolite, Permian gabbro intruding the Cariboo terrane, gabbro sills and dikes between Keithley and Rollie creeks and gabbro intrusions in the Downey succession north of Mount Barker. **b)** Neoproterozoic to Cambrian metavolcanic rocks near Badger Peak, metavolcanic rocks in the Harveys Ridge succession south of Frank Creek, metavolcanic rocks in the Harveys Ridge succession north of Cariboo Lake, sheared gabbro and metavolcanic rocks southwest of Keithley Creek, and metavolcanic rocks along the ridge containing Mount Barker.

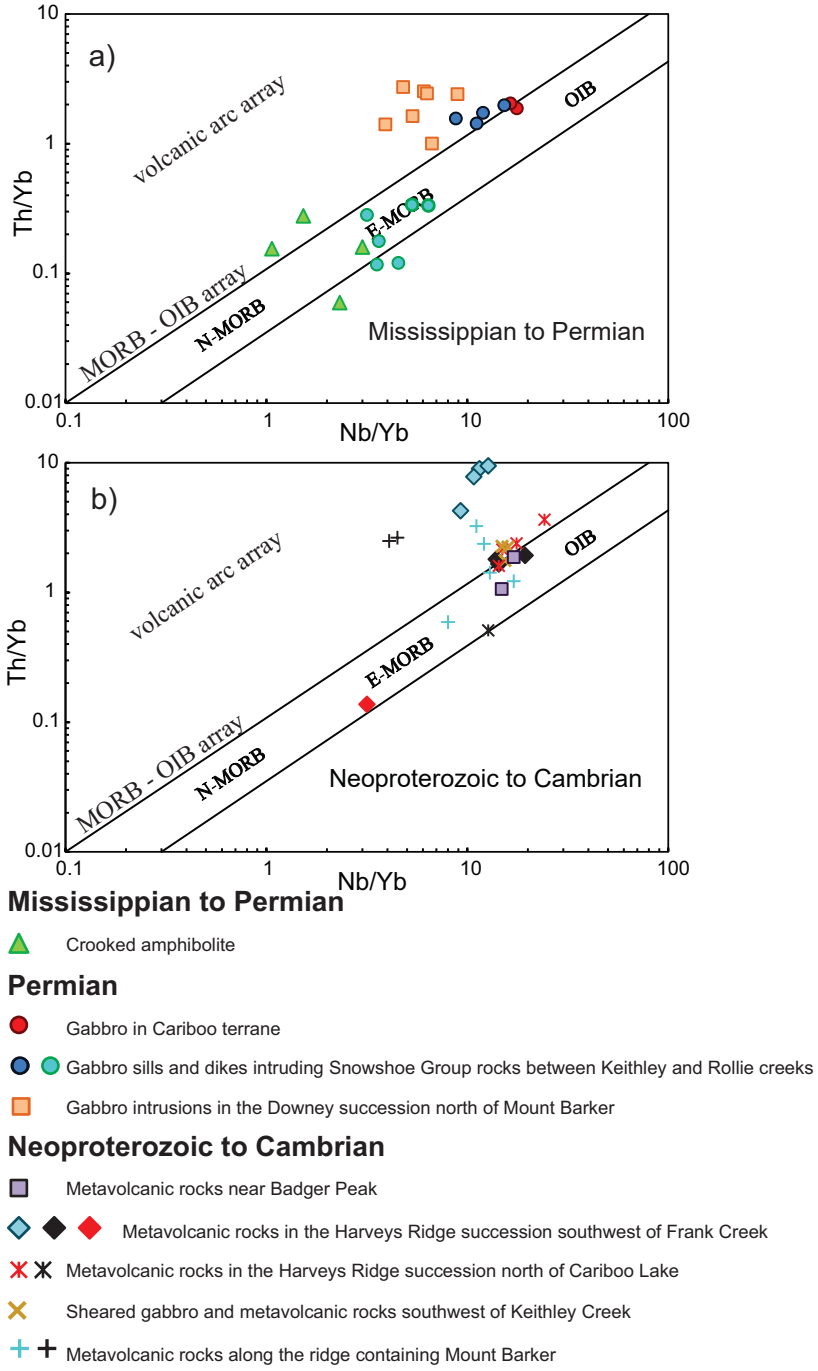

Fig. 7. Tectonic discrimination diagram of Pearce (2008). **a)** Mississippian to Permian rocks of the Crooked amphibolite, Permian gabbro intruding the Cariboo terrane, gabbro sills and dikes between Keithley and Rollie creeks, and gabbro intrusions in the Downey succession north of Mount Barker. **b)** Neoproterozoic to Cambrian metavolcanic rocks near Badger Peak, metavolcanic rocks in the Harveys succession south of Frank Creek, and metavolcanic rocks in the Harveys Ridge succession north of Cariboo Lake, sheared gabbro and metavolcanic rocks southwest of Keithley Creek, and metavolcanic rocks along the ridge containing Mount Barker.

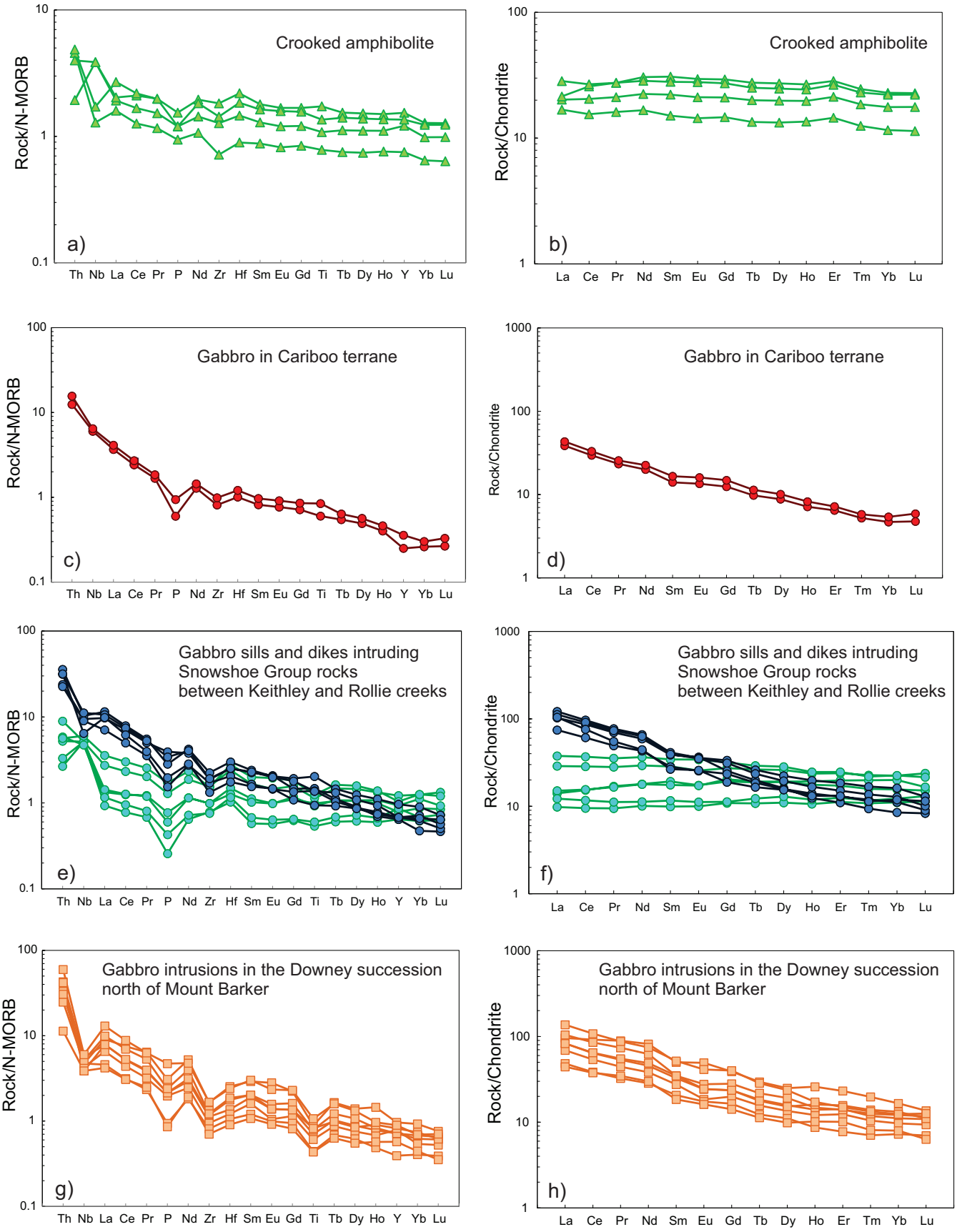

Fig. 8. a-h) Rare earth element plots for igneous and volcanic rocks in Figures 6 and 7.

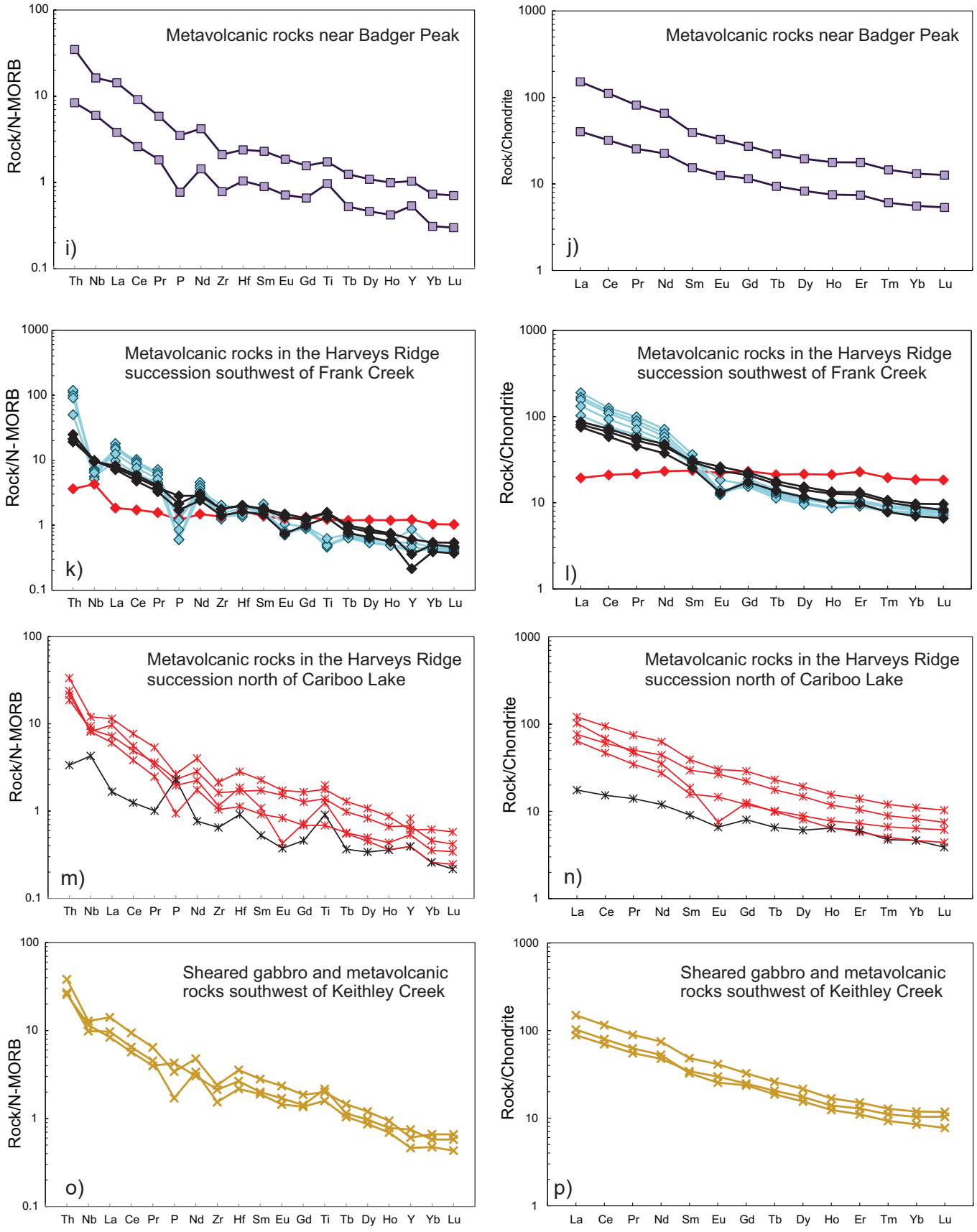

Fig. 8 continued. i-p) Rare earth element plots for igneous and volcanic rocks in Figures 6 and 7.

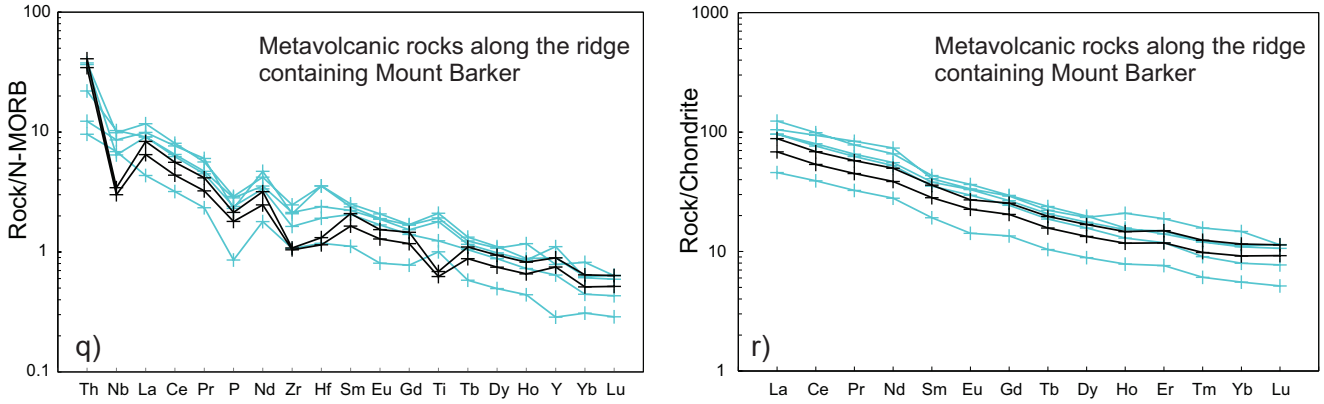

Fig. 8 continued. q-r) Rare earth element plots for igneous and volcanic rocks in Figures 6 and 7.

body (Fig. 3) returned similar ages of ca. 280 Ma. All the gabbros share similar characteristics and are assumed to be of the same age. Trace element data suggest these rocks are predominantly basaltic in composition with one being alkali basalt (Fig. 6a). All samples show similar trends, clustering in the volcanic arc array (Fig. 7a) and displaying arc-like trends on REE and extended REE plots, with negative Nb and Ti anomalies, enriched light REE, and depleted heavy REE (Figs. 8g, h).

5.3. Neoproterozoic to Cambrian

5.3.1. Metavolcanic rocks near Badger Peak

Several horizons of chlorite schist and finely crystalline foliated gabbro outcrop along the ridge immediately south of Badger Peak (Fig. 3) and plot as alkaline basalts (Fig. 6b). Gabbro at Badger Peak has OIB-like REE abundances similar to gabbro in the Cariboo terrane (Fig. 7b) whereas the chlorite schists, here assumed to be metavolcanic, display higher REE abundances (Figs. 8i, j).

5.3.2. Metavolcanic rocks in the Harveys Ridge succession southwest of Frank Creek

Initial mapping of chlorite-actinolite schist, tuffs, lapilli tuffs, and pillowed volcanic rocks in the Harveys Ridge succession southwest of Frank Creek recognized mafic and more felsic varieties, which is borne out by geochemistry. Most straddle the basalt to basaltic andesite fields but one plots as a basalt and there is an alkali basalt cluster (Fig. 6b). The basaltic andesites fall within the volcanic arc array, the one sample of basaltic composition plots in the E-MORB field and the alkali basalts plot as OIB (Fig. 7b). Samples that straddle the basalt to basaltic-andesite composition have REE abundances more compatible with island arc volcanic rocks, particularly as displayed by the negative Ti and Nb anomalies (Figs. 8k, l). The single basalt sample displays flat, MORB-like REE abundances (Figs. 8k, l), whereas the alkali basalts have REE levels compatible with ocean island basalts (Figs. 8k, l).

5.3.3. Metavolcanic rocks in the Harveys Ridge succession north of Cariboo Lake

Dark green metavolcanic rocks in the form of chlorite schist form isolated outcrops to mappable bodies up to several 100 m thick in the Harveys Ridge succession north of Cariboo Lake (Fig. 3). These have similar trace and REE abundances as the alkali basalts southwest of Frank Creek (Figs. 6b, 7b, 8m, n). One sample displays abundances that deviate significantly from the other samples (black symbol, Figs. 6, 7). This sample is highly deformed and altered with SiO_2 less than 40%, alkali metal contents of approximately 0.01% and volatiles of more than 18%.

5.3.4. Sheared gabbro and metavolcanic rocks southwest of Keithley Creek

Southwest of Keithley Creek is a fault-bounded package of highly strained, garnet-bearing chlorite-actinolite schist and gneiss that may have originated as gabbro. Trace element abundances suggest these rocks have compositions consistent with alkali basalt (Fig. 6b) and that they plot in the OIB portion of the MORB-OIB array (Fig. 7b) suggesting a within-plate setting. Rare earth element and extended REE are consistent with these data (Figs. 8o, p).

5.3.5. Metavolcanic rocks along the ridge containing Mount Barker

Dark green chlorite schists of metavolcanic origin exposed along the ridge containing Mount Barker (Fig. 3) display basaltic to alkali basalt bulk compositions (Fig. 6b). These rocks form one cluster within the volcanic arc array (black) and another suggesting within-plate abundances (blue; Fig. 7b). This is supported by REE and extended REE distributions (Figs. 8q, r).

6. Sm-Nd isotopic geochemistry

Using the geochronologic data presented above, we use a crystallization age of ca. 280 Ma for three of the samples and assume that sample (01FFe-3-1) is of the same age (Table 3; Fig. 9). Two samples from gabbro sills and dikes that intrude

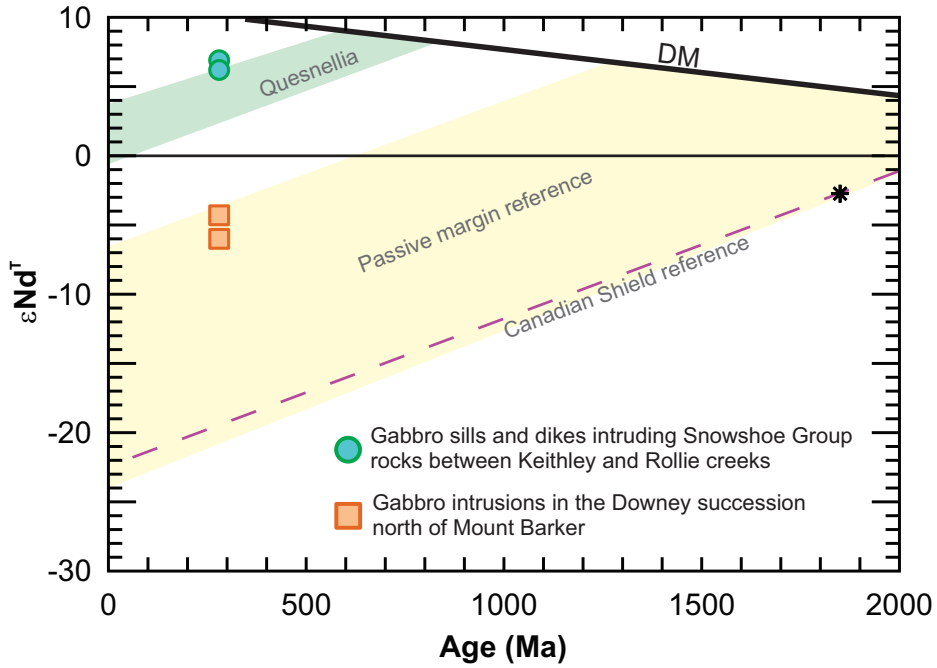

Fig. 9. Age vs. eNd^T. For comparison, Quesnellia reference (green band) constructed using whole rock Sm-Nd isotopic data from intrusive rocks (n = 6 $^{147}Sm/^{144}Nd = 0.112$) in Hogem batholith (Jurassic-Cretaceous; 200 to 130 Ma; Ootes et al., 2020). DM – depleted mantle evolutionary curve as defined by Goldstein et al. (1984). Passive margin reference constructed using whole rock Sm-Nd isotopic data (n = 8 $^{147}Sm/^{144}Nd = 0.112$) from sedimentary rocks of the Road River Group (Silurian; ca. 425 Ma) in the Mackenzie Mountains, NT (data in Rasmussen et al., 2023). Canadian Shield reference line constructed using average of 67 whole rock Sm-Nd isotopic data (n = 67, average $^{147}Sm/^{144}Nd = 0.11$), from igneous rocks in Wopmay orogen of the western Canadian Shield, NT (data from Jackson et al., 2022). Asterix at ca. 1.85 Ga represents youngest intrusive rocks exposed in the western Canadian Shield, where most exposures are Neoarchean to Paleoproterozoic. The line represents approximate maximum eNdT at a given time for magmas derived exclusively from Canadian Shield sources.

Downey succession rocks between Keithley and Rollie creeks have Sm-Nd isotopic ratios that indicate derivation from a mantle source more primitive than Quesnel terrane. In contrast, two samples from the large gabbro body intruding the Downey succession north of Mount Barker has Sm-Nd isotopic ratios that are more evolved, suggesting derivation from continental lithosphere.

7. Discussion

Neoproterozoic to Cambrian rocks in the Snowshoe Group can be grouped into two broad packages: 1) metavolcanic rocks in the Downey succession which include metavolcanic rocks along the ridge containing Mount Barker and sheared gabbro and metavolcanic rocks southwest of Keithley Creek (Fig. 6b); and 2) metavolcanic rocks in the Harveys Ridge succession or Transitional Harveys Ridge succession, which include metavolcanic rocks near Badger Peak, metavolcanic rocks in the Harveys Ridge succession north of Cariboo Lake, and metavolcanic rocks in the Harveys Ridge succession southwest of Frank Creek (Fig. 6b).

Volcanic rocks in the Downey succession generally have trace element levels indicating alkali basalt bulk compositions and trace element and REE abundances that define OIB (within-plate) eruptive settings. The only exception are several localities along Mount Barker that have compositions defining basalt compositions and signatures suggesting derivation from arc-related volcanism. Similarly, volcanic rocks in the Harveys Ridge succession generally have alkali basalt bulk compositions and also show OIB (within-plate) tectonic settings. Although some samples from south of Frank Creek follow this trend, others fall outside this cluster with E-MORB (basalt) and volcanic arc (basaltic andesite) characteristics.

Pearce (2008) noted that modern MORB volcanic rocks erupting at a continental margin can show distributions of data points within Th/Yb versus Nb/Yb space that spread from the MORB array into the volcanic-arc array along a line with a positive slope, similar to what we see with data from volcanic rocks south of Frank Creek. This results from contamination of MORB basalts by continental lithosphere, although it is difficult to maintain a basaltic composition and produce such a magma by mixing with continental lithosphere. Although sparse, our data from volcanic rocks south of Frank Creek do not show the transitional spread such as described by Pearce (2008) but rather define distinct clusters suggesting eruption of discrete magma types. Taken at face value, these data support coeval eruption of MORB and arc lavas, which suggests a Neoproterozoic-Cambrian back-arc setting along this portion of the Ancestral North American margin. Alternatively these volcanic rocks could have been sourced from lithosphere with arc characteristics and not an active arc environment.

Permian gabbros intrude the Snowshoe Group in two areas: between Keithley and Rollie creeks and north and northwest of Mount Barker. Although bulk compositions based on trace element data are identical for these two groups, which suggests they are part of the same igneous suite, other trace and REE data may imply two different magma sources. Gabbros between Keithley and Rollie creeks are of alkali basalts suggesting eruption within an OIB (i.e., within-plate) setting whereas those with basaltic abundances form a grouping of E-MORB affinities. Gabbro in the Mount Barker area displays alkali basalt to predominantly basaltic compositions but defines a cluster in the volcanic arc array and REE abundances that support this. Taken together, the two groups could define a contamination trend from continental lithosphere as proposed by Pearce (2008) and this is supported by the more evolved nature of Mount Barker area gabbros based on Sm-Nd isotopes. Again, as with the volcanic rocks south of Frank Creek, the data points do not define a continuous spread between the two end members, which suggests distinct magma sources. If we simply accept the geochemical and geochronological data, both MORB and arc magmatism appear to have been active during the Early Permian along this part of the Ancestral North American margin. Again, it should be cautioned that this arc signature could also be inherited from a continental lithospheric source. Rocks of the Crooked Amphibolite have a N-MORB signature and are, in part, of similar age. Taken together, this would be consistent with a proposed back-arc setting along the western margin of Ancestral North America during the Permian (Ferri, 1997). Evidence for a late Paleozoic arc immediately outboard of the Ancestral North American margin has been documented elsewhere in the Canadian Cordillera (Nelson and Colpron, 2006; Ferri, 1997; Ferri and Friedman, 2026).

8. Summary

Legacy multigrain U-Pb zircon analysis on three samples of gabbro that intrude the Snowshoe Group (late Neoproterozoic to early Cambrian) in the Cariboo subterrane near Cariboo Lake returned ages of ca. 280 Ma. Geochemical and isotopic data defines two groups. One displays elemental concentrations suggesting derivation from an E-MORB and OIB (within-plate) source and having Sm-Nd isotopic abundances indicating the magmas originated from an immature, mantle source. The second has arc-like signatures and Sm-Nd isotopic levels that suggest derivation from more evolved continental lithosphere. These relationships would be consistent with a Permian back-arc setting along the western margin of Ancestral North America during the Permian. Lithogeochemical analysis of mafic volcanic rocks in the Snowshoe Group support coeval eruption of MORB and arc lavas, are consistent with an older (Neoproterozoic to Cambrian) back-arc setting.

Acknowledgments

We thank L. Ootes for helpful comments and providing the diagram used in Figure 9 and L. Aspler for thorough reviews of early versions of this paper.

References cited

Bichler, A., and Bobrowsky, P.T., 2001. Barkerville Project: Regional till geochemistry (93H/4, 5) and orientation (93A/14) studies. In: Geological Fieldwork 2000, British Columbia Ministry of Energy and Mines, British Columbia Geological Survey Paper 2001-1, pp. 383-396.

Bloodgood, M.A., 1990. Geology of the Eureka Peak and Spanish Lake map area. British Columbia Ministry of Energy, Mines and Petroleum Resources, British Columbia Geological Survey Paper 1990-3, 38 p.

Campbell, R.B., 1978. Quesnel Lake, British Columbia. Geological Survey of Canada Open File 574, 1:125,000 scale.

Colpron, M., 2020. Yukon terranes-A digital atlas of terranes for the northern Cordillera. Yukon Geological Survey. <https://data.geology.gov.yk.ca/Compilation/2#InfoTab>

Crowley, J.L., Schoene, B., and Bowring, S.A., 2007. U-Pb dating of zircon in the Bishop Tuff at the millennial scale. Geology, 35, 1123-1126.

Ferri, F., 1997. Nina Creek Group and Lay Range assemblage, north-central British Columbia: Remnants of Late Paleozoic and arc terranes. Canadian Journal of Earth Sciences, 34, 854-874.

Ferri, F., 2001a. Geological setting of the Frank Creek massive sulphide occurrence near Cariboo Lake, east-central B.C. In: Geological Fieldwork 2000, British Columbia Ministry of Energy and Mines, British Columbia Geological Survey Paper 2000-1, pp. 31-49.

Ferri, F., 2001b. Geology of the Frank Creek-Cariboo Lake area, central British Columbia (NTS 93A/11, 14). British Columbia Ministry of Energy and Mines, British Columbia Geological Survey Open File 2001-11, 1:25,000 scale.

Ferri, F., and Friedman, R., 2026. Age and geochemistry of middle to late Paleozoic volcanism along the western edge of Ancestral North America in north-central British Columbia. In: Geological Fieldwork 2025, British Columbia Ministry of Mining and Critical Minerals, British Columbia Geological Survey Paper 2026-01, pp. 183-201.

Ferri, F., and O'Brien, B., 2002. Preliminary Geology of the Cariboo Lake Area, central British Columbia (093A/11, 12, 13 and 14). In: Geological Fieldwork 2001, British Columbia Ministry of Energy and Mines, British Columbia Geological Survey Paper 2002-1, pp. 59-82.

Ferri, F., and O'Brien, B., 2003. Geology of the Cariboo Lake area, Central British Columbia. British Columbia Ministry of Energy and Mines, British Columbia Geological Survey Open File 2003-01, 1:50,000 scale.

Ferri, F., and Schiarizza, P., 2006. Reinterpretation of the Snowshoe Group stratigraphy across a southwest-verging nappe structure and its implications for regional correlations within the Kootenay terrane. In: Colpron, M., and Nelson, J.L., (Eds.), Paleozoic Evolution and Metallogeny of Pericratonic Terranes at the Ancient Pacific Margin of North America, Canadian and Alaskan Cordillera. Geological Association of Canada, Special Paper 45, pp. 415-432.

Goldstein, S.L., O'Nions, R.K., and Hamilton, P.J., 1984. A Sm-Nd isotopic study of atmospheric dusts and particulates from major river systems. Earth and Planetary Science Letters, 70, 221-236.

Hamilton, P.J., O'Nions, R.K., Bridgwater, D., and Nutman, A., 1983. Sm-Nd studies of Archaean metasediments and metavolcanics from West Greenland and their implications for the Earth's early history. Earth and Planetary Science Letters, 62, 263-272.

Höy, T., and Ferri, F., 1998a. Zn-Pb deposits in the Cariboo subterrane, central British Columbia (93A/NW). In Geological Fieldwork 1997, British Columbia Ministry of Employment and Investment, British Columbia Geological Survey Paper 1998-1, pp.14-1-14-10.

Höy, T., and Ferri, F., 1998b. Stratabound base metal deposits of the Barkerville subterrane, central British Columbia (093A/NW). In: Geological Fieldwork 1997, British Columbia Ministry of Employment and Investment, British Columbia Geological Survey Paper 1998-1, pages 13-1-13-12.

Jackson, V.A., Ootes, L., Pierce, K., Bennett, V., Smar, L., Mackay, D., and Sandeman, H.A., 2022. Geology of the south-central Wopmay orogen, Northwest Territories (parts of NTS 86B, 86C, and 86D); Results from the South Wopmay Bedrock Mapping Project. Northwest Territories Geological Survey, NWT Open File 2017-10, 103 p.

Krogh, T.E., 1982. Improved accuracy of U-Pb zircon ages by the creation of more concordant systems using an air abrasion technique. Geochimica et Cosmochimica Acta, 46, 637-649.

Ludwig K.R., 2003. Isoplot 3.00, A Geochronological Toolkit for Microsoft Excel. University of California at Berkely.

Ootes, L., Jones, G., Schiarizza, P., Milidragovic, D., Friedman, R., Camacho, A., Luo, Y., Vezinet, A., Pearson, D.G., and Zhang, S., 2020. Geochronologic and geochemical data from northern Hogem batholith and its surroundings, north-central British Columbia. British Columbia Ministry of Energy, Mines and Low Carbon Innovation, British Columbia Geological Survey GeoFile 2020-01, 21 p.

Panteleyev, A., Bailey, D.G., Bloodgood, M.A., and Hancock, K.D., 1996. Geology and mineral deposits of the Quesnel River-Horsefly map area, central Quesnel trough, British Columbia. British Columbia Ministry of Employment and Investment, British Columbia Geological Survey Bulletin 97, 156 p.

Parrish, R., Roddick, J.C., Loveridge, W.D., and Sullivan, R.W., 1987. Uranium-lead analytical techniques at the geochronology laboratory, Geological Survey of Canada. In: Radiogenic Age and Isotopic Studies, Report 1, Geological Survey of Canada Paper 87-2, pp. 3-7.

Pearce, J.A., 2008. Geochemical fingerprinting of oceanic basalts with applications to ophiolite classification and the search for Archean oceanic crust. Lithos, 100, 14-48.

Pearce, J.A., 1996. A user's guide to basalt discrimination diagrams. In: Wyman, D.A., (Ed.), Trace Element Geochemistry of Volcanic Rocks: Applications for Massive Sulphide Exploration. Geological Association of Canada, Short Course Notes, 12, pp. 79-113.

Rasmussen, K.L., Falck, H., Elongo, V., Reimink, J., Luo, Y., Pearson, D.G., Ootes, L., Creaser, R.A., and Lecumberri-Sanchez, P., 2023. The source of tungsten-associated magmas in the northern Canadian Cordillera and implications for the basement. Geology, 51, 657-662.

Ray, G.E., Webster, I.C.L., Ross, K., and Hall, R., 2001. Geochemistry of auriferous pyrite mineralization at the Bonanza Ledge, Mosquito Creek mine and other properties in the Wells-Barkerville area, British Columbia. In Geological Fieldwork 2000, British Columbia Ministry of Energy and Mines, British Columbia Geological Survey Paper 2001-1, pp. 135-168.

Rees, C.J., 1987. The Intermontane-Omineca Belt boundary in the Quesnel Lake area, east-central British Columbia: Tectonic implications based on geology, structure and paleomagnetism. Ph.D. thesis; Carleton University, Ottawa, Ontario, 421 p.

Rees, C.J., and Ferri, F., 1983. A kinematic study of mylonitic rocks in the Omineca-Intermontane belt tectonic boundary in east-central British Columbia. In: Current Research, Geological Survey of Canada Paper 83-1B, pp. 121-125.

Schiarizza, P., 2024. Bedrock geology, Bonaparte Lake-Quesnel River parts of NTS 92P, 93A, 93B. British Columbia Ministry of Energy, Mines and Low Carbon Innovation, British Columbia Geological Survey Geoscience Map 2024-01, 1:125,000 scale.

Schiarizza, P., and Ferri, F., 2003. Barkerville terrane, Cariboo Lake to Wells: A new look at stratigraphy, structure and regional correlations of the Snowshoe Group. In Geological Fieldwork 2002, British Columbia Ministry of Energy and Mines, British Columbia Geological Survey Paper 2003-1, pp. 77-98.

Schmitz, M.D., and Schoene, B., 2007. Derivation of isotope ratios, errors, and error correlations for U-Pb geochronology using ^{205}Pb-^{235}U-(^{233}U)-spiked isotope dilution thermal ionization mass spectrometric data. Geochemistry, Geophysics, Geosystems, 8, article Q08006. <https://doi.org/10.1029/2006GC001492>

Stacey, J.S., and Kramer, J.D., 1975. Approximation of terrestrial lead isotope evolution by a two-stage model. Earth and Planetary Science Letters, 26, 207-221.

Struik, L.C., 1983a. Bedrock geology of Spanish Lake (93A/11) and parts of adjoining map areas, central British Columbia. Geological Survey of Canada Open File 920, 1:50,000 scale.

Struik, L.C., 1983b. Bedrock geology of Quesnel Lake (93A/10) and part of Mitchell Lake (93A/15) map areas, central British Columbia. Geological Survey of Canada Open File 962, 1:50,000 scale.

Sun, S.S., and McDonough, W.F., 1989. Chemical and isotopic systematics of oceanic basalts: Implications for mantle composition and processes. In: Saunders, A.D., and Norry, M.J., (Eds.), Magmatism in the Ocean Basins. Geological Society, London, Special Publication, 42, pp. 313-345.

Thirlwall, M.F., 2000. Inter-laboratory and other errors in Pb isotope analyses investigated using a ^{207}Pb-^{204}Pb double spike: Chemical Geology, 163, 299-322.